ARTICLE

Atmospheric pressure plasma jet-assisted decolorization of malachite green and natural orange dye

Dominic B. Soriano, Mac Michael M. Rubio*, and Giovanni M. Malapit

Department of Physical Sciences, College of Science, University of the Philippines Baguio, Baguio City, Benguet 2600, Philippines

ABSTRACT

This study investigates the decolorization of aqueous solutions of malachite green (MG) and natural orange dye using direct and indirect treatments with a non-thermal atmospheric-pressure plasma jet (APPJ). In the direct treatment, the dye solutions were exposed directly to the plasma plume, whereas the indirect treatment was carried out using plasma-activated water (PAW) generated by exposing water to the plasma jet prior to its application to the dye solutions. Dye decolorization efficiencies were quantified using UV–Vis spectroscopy by monitoring changes in the characteristic absorbance of the dyes, from which concentrations were derived, during treatment. The direct plasma treatment achieved maximum decolorization efficiencies of $95.32 \pm 0.29\%$ for MG and $92.47 \pm 1.29\%$ for natural orange dye within 45 minutes. In contrast, the indirect treatment using 60-minute PAW exposure resulted in decolorization efficiencies of $19.20 \pm 2.60\%$ for MG and $24.90 \pm 1.35\%$ for natural orange dye. Physicochemical parameters such as pH, conductivity, total dissolved solids (TDS), and dissolved oxygen (DO) were significantly altered due to the generation of reactive oxygen and nitrogen species (RONS) during direct plasma treatment, as identified by optical emission spectroscopy. Kinetic analyses revealed that the decolorization of MG and natural orange dye followed second-order kinetics under direct plasma treatment. These findings highlight the potential of APPJ-based treatments as a promising strategy for effective dye wastewater remediation.

INTRODUCTION

Water resources are increasingly threatened by the rapid growth of the global population and industrial activities. Industrial and domestic effluents are major sources of water contamination. An estimated 56% of global freshwater withdrawals ultimately return as industrial, agricultural, and domestic wastewater. Approximately 70% of wastewater is discharged directly into the environment without proper treatment (Peramune et al. 2022). Increasing quantities of wastewater pollutants are produced worldwide from the textile, cosmetics, paper, rubber, leather, and printing industries (Younis et al. 2021). The textile industry is a major contributor to water contamination, particularly through effluents generated during the washing and cleaning of colored textile fibers. The released wastewater contains not only colored dye but also metallic particles, suspended solids, high chemical oxygen demand, and extreme pH values. Textile wastewater can pose significant health risks to humans due to the carcinogenic properties of certain dyes and the toxic compounds they produce, raising serious environmental concerns (Pattnaik et al. 2018; Wang et al. 2022).

Most textile industries use synthetic colorants such as azo, anthraquinone, triarylmethane, and reactive dyes. These dyes are chemically stable under both aerobic and anaerobic conditions, making them difficult to degrade and a significant environmental concern (Vasu et al. 2020). One of these triarylmethane dyes is malachite green (MG), commonly used in the dyeing and printing of fibers, coloring paints, plastics, among other applications. It is also used in aquaculture as an effective biocide. In the Philippines, MG has been used as a disinfectant in grow-out ponds for *Penaeus monodon* (the giant tiger prawn) by aquaculture operators (Cruz-Lacierda et al. 2000). However, it has been banned in several countries, particularly in the Philippines, due to its harmful effects on the immune and reproductive systems of mammals and other animals. Its carcinogenic potential is of significant concern, as MG has been identified as a tumor promoter (Wang et al. 2020).

The concentration of MG reported near industrial discharge sites, aquaculture facilities, and polluted water bodies ranges from 0.1 to 5 mg/L. This is concerning because concentrations exceeding 2 µg/g (equivalent to 2 mg/L) can pose health risks to humans. The low biodegradability and intense coloration of MG significantly impede photosynthesis in aquatic ecosystems, potentially leading to severe ecological imbalances (Ouzar et al. 2024).

*Corresponding author
Email Address: **mmrubio1@up.edu.ph**
Date received: 21 August 2025
Dates revised: 23 February 2026, 11 June 2026
Date accepted: 12 July 2026
DOI: https://doi.org/10.54645/2026192AJD-53

KEYWORDS

atmospheric pressure plasma jet, plasma-activated water, decolorization, reactive species, malachite green, natural orange dye

Due to the environmental issues caused by commercially available synthetic dyes, the demand for using natural dyes as an alternative is increasing. Natural dyes are preferred because they are inexpensive, widely applicable, and extractable using environmentally benign methods from natural resources (Bhandari et al. 2020). Color intensity depends on which part of the plant is used. Lighter hues are extracted from fruits and leaves, while the darker colors are derived from the seeds, roots, and barks. Abra, a province in the Cordillera region of the Philippines, is noted for its production of natural dyes, such as the orange dye derived from annatto seeds. Annatto dye has an enormous number of applications in food, cosmetic, and textile industries (Devi et al. 2013). Although natural dyes are generally considered safe and eco-friendly, the chemical compounds used in textile dyeing and processing can still generate pollutants (Ouzar et al. 2024).

Several methods have been employed to eliminate the dye effluent from the wastewater such as ultrafiltration, coagulation, membrane separation, and biological treatment. However, these conventional wastewater treatment methods are often ineffective against these dyes due to their stable chemical structures and may generate harmful by-products. Advanced oxidation processes that generate reactive oxygen species (ROS) and reactive nitrogen species (RNS) have achieved more effective dye removal (Vasu et al. 2020; Kumar et al. 2022; Attri et al. 2016).

Non-thermal plasma is an alternative tool for the oxidation of organic contaminants from water due to the generation of various ROS and RNS. Plasma in contact with water can effectively treat various organic pollutants, including synthetic dyes. During direct treatment, the dye solution is exposed to plasma factors such as high-energy electrons, short- and long-lived ROS and RNS, UV emission, and electric fields, which play a significant role in dye decolorization and degradation. For example, needle-type non-thermal direct atmospheric-pressure plasma jets have been widely employed for the treatment of dye-contaminated solutions, including methylene blue, methyl orange, and Congo red. These plasma jets generate a variety of ROS, which play a crucial role in the decolorization and degradation of dye molecules (Attri et al. 2016). On the other hand, indirect treatment using plasma-activated water (PAW) emerged as a promising medium for wastewater treatment and dye decolorization and degradation due to its ability to generate a diverse range of ROS and RNS without the addition of chemical oxidants. These reactive species promote the oxidation and breakdown of organic pollutants such as dyes, pesticides, and pharmaceutical compounds present in wastewater. Previous studies have demonstrated that PAW can effectively degrade dye molecules when mixed with contaminated solutions, achieving substantial pollutant removal over extended treatment periods (Kumar and Saxena 2026, preprint; Kumar, 2023; Kumar et al. 2022; Zhou et al. 2020).

Efficient removal of dyes from wastewater is essential for mitigating adverse environmental impacts, reducing the persistence of colored effluents, and improving water quality. Accordingly, this study investigated the potential of both direct atmospheric pressure plasma jet (APPJ) treatment and indirect plasma-activated water (PAW) treatment for the decolorization of MG and natural orange as a step toward developing an effective, environmentally friendly, and sustainable plasma-based technology for dye wastewater treatment.

MATERIALS AND METHODS

Atmospheric Pressure Plasma Jet (APPJ) System

The APPJ system used in this study is a modified version of that described by Malapit and Baculi (2022). The schematic representation and actual set-up of the APPJ are shown in Figure 1.

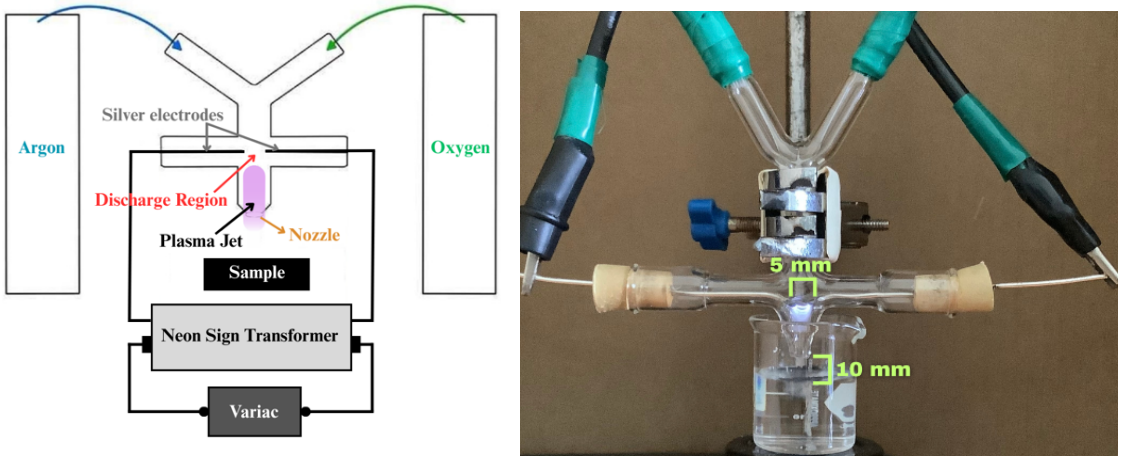

Figure 1: (**a**) Schematic diagram and the (**b**) APPJ experimental setup for direct treatment and PAW generation

An atmospheric pressure plasma discharge was generated in a customized glass chamber equipped with two gas inlets and two openings for a pair of 1.5 mm electrodes, each made from 6-inch silver rods (99.5% purity) and secured with rubber stoppers. The electrodes were powered by a 60 Hz, 450 W neon-sign transformer delivering 15 kV and 30 mA. To ensure reproducible experimental conditions, the transformer was connected to a variable autotransformer (variac) to precisely control the input voltage and maintain a stable, uniform plasma plume throughout the direct treatment and PAW generation. A controlled mixture of argon and oxygen gases (99.9% purity) served as the feed gases, with flow rates regulated by a flowmeter. The plasma plume was emitted from a nozzle with an inner diameter of 5 mm.

Plasma Discharge Characterization

An Ocean Optics optical emission spectroscopy (OES) setup was used to analyze the plasma and identify reactive species generated during treatment. The OES system was calibrated for both wavelength and relative intensity response using a broad-spectrum reference light source to ensure consistent detector sensitivity and alignment across the measured range. Plasma emission was collected via an optical fiber mounted on a holder, with the lens positioned directly in front of the plasma discharge region. The optical spectrometer transmitted the acquired data to a PC, where spectral lines were displayed using OceanView software. Subsequently, plasma species were identified using Spectrum Analyzer 1.97, a software program developed and designed for optical spectra display, recognition, and analysis. Species identification was performed by matching the observed emission

peaks to the software's integrated database, which includes the National Institute of Standards and Technology (NIST) 5.1 database for atomic lines and a dedicated database for molecular bands (e.g., OH, N_2, O_2) (Navrátil et al., 2006).

The electron temperature was calculated using the built-in function of Spectrum Analyzer, based on the intensities of selected spectral lines. Plasma gas temperature was measured with a Cooper-Atkins K-type thermocouple (50332-K) positioned at the periphery of the plasma plume which is approximately 5mm from the discharge axis to minimize errors due to charged particle interactions and electromagnetic interference. Temperature readings were recorded once they reached a steady state to confirm whether the gas temperature was consistent with that of a cold atmospheric pressure plasma.

Preparation of Dye Aqueous Solutions

A 100 ppm malachite green (MG) solution was prepared by accurately weighing 100 mg of MG on an analytical balance and dissolving it in distilled water to obtain a final volume of 1000 mL at room temperature. The solution was stored in a sealed container and wrapped in aluminum foil to prevent light exposure. The natural orange dye from annatto seeds was procured from Revival Dye, a natural dye supplier based in Abra, Benguet. To remove coarse particles that could introduce impurities during solution preparation, the dye powder was passed through a 100-micron sieve. A 600 ppm orange dye stock solution was prepared by dissolving 600 mg of dye in 50 mL of boiling distilled water and stirring for 20 minutes with a magnetic stirrer. The solution was then diluted with distilled water to a target concentration of 750 ppm, followed by an additional 10 minutes of stirring at room temperature. The prepared solution was stored in a sealed container and wrapped in foil to protect it from light.

Production of Plasma-Activated Water for Indirect Treatment

To generate plasma, argon (Ar) and oxygen (O_2) gases were supplied at flow rates of 2.5 and 1.0 L·min^{-1}, respectively. The Ar/O_2 gas mixture was selected based on both plasma stability considerations and reactive species generation efficiency (Pineda et al. 2025). Argon, a noble gas, was used as the primary carrier gas because its chemical inertness and low breakdown voltage are critical in maintaining stable and uniform plasma discharge. The addition of oxygen promotes the generation of highly oxidative reactive oxygen species (ROS), which are primarily responsible for dye molecule decolorization and degradation. The selected flow rates were determined through preliminary optimization experiments, where multiple gas ratios were evaluated. The chosen mixture yielded the highest decolorization efficiency (calculated using Eq. 1; Silva et al. 2021) while maintaining discharge stability.

$$Decolorization\ Efficiency\ (\%) = \frac{C_o - C_t}{C_o} \times 100 \quad \text{(Equation 1)}$$

where C_o is the initial concentration at time zero and C_t is the final concentration of the samples at time t.

A 20 mL beaker containing 15 mL of distilled water was positioned 10 mm below the APPJ nozzle and exposed to the plasma plume. The plasma plume was in direct contact with the surface of the water to facilitate the treatment process. Treatments were conducted for 5, 10, 15, 25, 35, and 60 minutes, with three replicates for each duration. Following each treatment, physicochemical characterization was performed on the generated PAW. Immediately thereafter, an 8 mL aliquot of the characterized PAW was combined with 8 mL of dye solution in a test tube. The mixture was manually agitated for 1 minute using a consistent up-and-down motion to ensure immediate and uniform mixing. This method was chosen to allow reactive species to interact with the dye instantly while avoiding the introduction of excess air. The prepared mixtures were then stored for 10 days to monitor changes. The initial storage temperature was recorded at 21°C, consistent with the ambient room temperature of the laboratory at the time of measurement. Moreover, all samples were kept inside a light-proof box to prevent possible structural modifications.

Direct Plasma Treatment

For the direct treatment of both MG and natural orange dye aqueous solutions, the same parameters as those used for PAW generation were applied. Argon (Ar) and oxygen (O_2) gases were supplied at flow rates of 2.5 and 1.0 L·min^{-1}, respectively. A 15 mL beaker containing 15 mL of dye solution was positioned 10 mm below the APPJ nozzle and exposed to the plasma plume. The surface of the dye solutions was in direct contact with the plasma plume to ensure that reactive species were transferred directly and interacted with the samples. Treatments were conducted for 5, 10, 15, 25, 35, and 45 minutes, with three replicates for each duration. All treated solutions were stored in a light-proof box to prevent light-induced degradation.

Physicochemical Properties of Direct Plasma-Treated Dye Solutions

The pH, electrical conductivity, total dissolved solids (TDS), and dissolved oxygen (DO) of direct plasma-treated dye solutions were measured before and after the decolorization process to assess the effects of plasma on their physicochemical properties.

pH was measured using a benchtop pH meter to evaluate its influence on dye decolorization, while electrical conductivity was determined using a LAQUAtwin conductivity meter to assess how plasma discharge enhances ionic mobility in the solution. TDS was measured with a portable TDS meter to quantify dissolved inorganic salts and organic matter, and DO was determined using a dissolved oxygen meter to evaluate oxygen concentration in the samples. All measurements were performed in triplicate to ensure reliability and reproducibility.

Measurement of Dye Decolorization using UV-Vis Spectroscopy

A Shimadzu UVmini-1240 UV-Vis spectrophotometer was used to determine the concentrations of MG and natural orange dye solutions before and after decolorization. For PAW–dye mixtures (1:1 ratio), measurements were taken after 10 days of storage for each treatment time. For direct plasma treatment, concentrations of untreated and treated solutions were measured immediately to evaluate treatment effectiveness. Standard calibration curves were used to determine sample concentrations from absorbance values, with the absorbance–concentration relationship expressed in Eq. 2.

$$y = mx + b \quad \text{(Equation 2)}$$

where y is the absorbance, m is the slope of the calibration curve, x is the concentration of the dye solution, and b is the y-intercept of the calibration curve. Additionally, the decolorization efficiency was calculated using Eq. 1.

Dye Decolorization Kinetic Models

Dye decolorization kinetics describe the rate at which decolorization reactions proceed and provide a framework for assessing how quickly a dye is removed during treatment. Kinetic analysis describes the time-dependent behavior and breakdown of dye molecules during direct plasma treatment.

The kinetic study was evaluated using the zero (Eq. 3), first (Eq. 4), and second (Eq. 5) order kinetic models of the linear type.

$$C_t = -k_o t + C_o \quad \text{(Equation 3)}$$

$$ln\ C_t = -k_1 t + ln\ C_o \quad \text{(Equation 4)}$$

$$\frac{1}{C_t} = k_2 t + \frac{1}{C_o}$$

(Equation 5)

where C_o and C_t are the initial concentration and final concentration after time t, respectively. k_0, k_1, and k_2, are the rate constants for zero order, first order, and second order equations, respectively. Graphs of C_t *vs.* t, $ln\ C_t$ *vs.* t, and $\frac{1}{C_t}$ *vs.* t were plotted to check whether the dye decolorization of each dye solution obeys zero, first, or second order kinetics. The half-lives of MG and natural orange dye solutions during the direct treatment were also calculated using the order of kinetics equation. All measurements were performed in triplicate to ensure reliability and reproducibility.

Statistical Analyses

Statistical analyses were performed using the Statistical Tool for Agricultural Research (STAR) software. One-way analysis of variance (ANOVA) was employed to evaluate significant differences among treatment times. When the ANOVA indicated significant effects, Tukey's Honest Significant Difference (HSD) post hoc test was conducted to identify pairwise differences between treatment means. Results are presented as mean ± standard deviation, and all statistical tests were evaluated at a significance level of $p < 0.05$.

RESULTS AND DISCUSSION

Plasma Generation and Characterization

A plasma jet was generated using a gas mixture of argon (Ar) and oxygen (O_2) gases. The plasma exhibited a bluish-pink, nearly uniform glow, attributed to the higher argon content. This observation is consistent with the findings of Jitsomboonmit et al. (2012), who reported similar filamentary discharges and arc currents around electrode edges under comparable operating conditions.

The reactive species generated in the plasma discharge were identified using optical emission spectroscopy (OES), with the wavelength–intensity profiles shown in Figure 2. Excited species such as hydroxyl radical (OH), atomic nitrogen (N I), atomic oxygen (O I), and neutral argon (Ar I) were observed. For example, OH I radical peaks were observed at 306.36 nm and 308.90 nm. N I was observed at 737.85 nm and 810.57 nm while Ar I was detected at 772.42 nm and 791.64 nm. O I was also observed at 210.08 nm and 842.62 nm. These ranges of observed emission lines are consistent with previously reported optical emission spectra of reactive oxygen and nitrogen species in atmospheric pressure plasma (Vasu et al. 2020; Kumar et al. 2022).

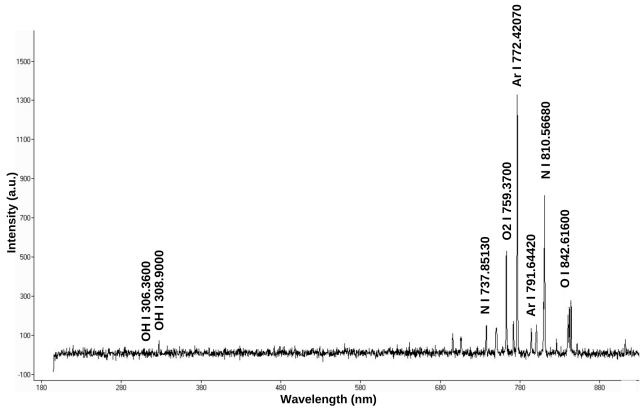

Figure 2: Optical Emission Spectra of the Argon-Oxygen Plasma

Using the built-in function of the spectrum analyzer software, the electron temperature was calculated to be 12,655 K (1.09 eV), while the gas temperature, measured with a Cooper-Atkins 50332-K thermocouple (probe diameter: 3.2 mm) positioned at the plume periphery (5 mm from the discharge axis), was 434.85 K (0.04 eV). The high electron temperature promotes plasma chemistry and reactive species generation, while the low gas temperature minimizes thermal effects (Baculi et al. 2023). This thermal non-equilibrium, characteristic of cold atmospheric pressure plasma, is key to introducing reactive species into aqueous solutions without causing thermal damage to the target molecules.

Dye Decolorization under Direct Plasma Treatment

For the direct plasma treatment, the initial concentrations (C_0) of the dye solutions were 750 ppm and 100 ppm for natural orange dye and malachite green, respectively. These concentrations were determined from the calibration curve using Eq. 2, which estimates the concentration from the measured absorbance. Figure 3 presents the decolorization efficiency of direct plasma treatment for each dye solution. After 45 min of treatment, the highest decolorization efficiencies were achieved, reaching 92.47 ± 1.29% for the natural orange dye and 95.32 ± 0.29% for MG. These values were statistically significantly different from those observed at the earlier treatment times. During direct plasma exposure, both long-lived and short-lived reactive species were generated, including hydroxyl radicals (•OH), singlet oxygen (O), atomic nitrogen (N), nitrate (NO_3^-), nitrite (NO_2^-), ozone (O_3), and hydrogen peroxide (H_2O_2). These reactive species dissolved into the solution to form potent acids and highly oxidative agents, attacking the chemical bonds of the dye molecules and leading to their decolorization and possible structural modifications. This process is confirmed by the OES results presented above and is consistent with previous reports (Vasu et al., 2020; Kumar et al., 2022). Figure 4 presents the visible color changes in the dye solutions following treatment. The pronounced decrease in color intensity corresponds to the high decolorization efficiencies, further confirming the effectiveness of direct plasma treatment in decolorizing both dyes and potentially altering their molecular structures.

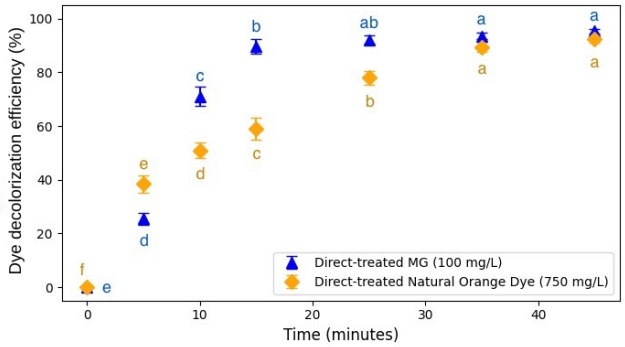

Figure 3: Dye decolorization efficiency of direct plasma treatment on the natural orange dye and MG aqueous solutions

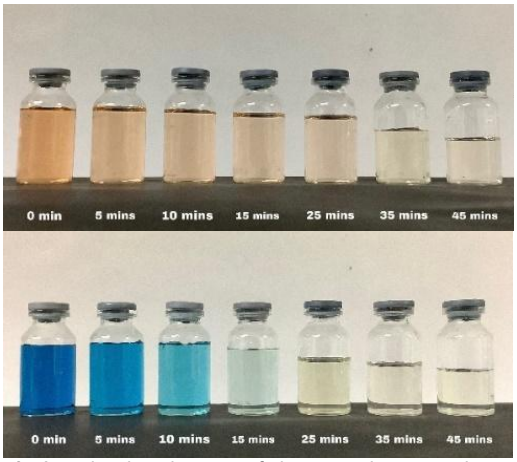

Figure 4: Actual color changes of the natural orange dye and MG aqueous solutions after direct plasma treatments

The short- and long-lived ROS and RNS generated during the direct treatment of the dye solutions, along with their possible reaction pathways, are presented below (Vasu et al., 2020; Kumar et al., 2022).

$$\cdot OH + \cdot OH \rightarrow H_2O_2 \text{ (Hydrogen Peroxide)}$$

$$2NO_2 + H_2O \rightarrow NO_3^- + NO_2^- + 2H^+ \text{ (Nitrate)}$$

$$NO + \cdot OH \rightarrow NO_2^- \text{ (Nitrite)}$$

$$O + O_2 + M \rightarrow O_3 + M \text{ (Ozone)}$$

$$H_2O + e^- \rightarrow \cdot OH + H^+ + e^- \text{ (Hydroxyl Radicals)}$$

$$NO + O_2^- \rightarrow ONOO^- \text{ (Peroxynitrite Acid)}$$

$$ONOO^- + H^+ \leftrightarrow ONOOH \text{ (Peroxynitrous Acid)}$$

The primary carotenoids in annatto orange dye are bixin and norbixin. Bixin, the most abundant pigment in annatto seeds (Aluko, 2024), is highly sensitive to light, with a reported half-life of 462 days in the dark and only 6 days under visible light. Norbixin has also been reported to be light-sensitive (Gallardo Cabrera & Rojas Barahona, 2015). Carotenoids possess a system of conjugated double bonds, making them susceptible to degradation under various factors such as temperature, light, oxygen, and pH (Gallardo Cabrera & Rojas Barahona, 2015). These factors contribute to the breakdown or rearrangement of the dye's chemical bonds. Furthermore, UV emission during plasma treatment increases the vulnerability of carotenoids to photo-oxidation. In addition, based on previously reported pathways, it is proposed that key reactive species, such as hydroxyl radicals (•OH), singlet oxygen (O), atomic nitrogen (N), nitrate (NO_3^-), nitrite (NO_2^-), ozone (O_3), and hydrogen peroxide (H_2O_2) attack dye molecules and promote decolorization and structural modifications (Vasu et al., 2020; Kumar et al., 2022).

On the other hand, based on the degradation pathways previously proposed by Oladoye et al. (2023), two ozonolytic mechanisms may be involved: (1) the generation of reactive radicals, particularly hydroxyl radicals, which attack the dye molecules, and (2) the direct reaction of molecular ozone with the dyes. These processes are believed to disrupt the chromophoric structure of MG and potentially alter other chemical bonds within the molecule. Ozone and hydroxyl radicals with high oxidation potential of 2.0 V and 2.8 V, respectively, are powerful enough to attack the C=C segment, resulting in the breakdown of the chemical structure of MG. Reportedly, when the hydroxyl radical attacks the central carbon of MG, this leads to the cleavage of the C-C bond and the N,N-dimethylaminobenzyl group, and intermediate compounds form (p-dimethylamino phenol and 4-(N,N-dimethylamino) methylbenzylone). The continued attack of hydroxyl radical on these intermediates leads to the formation of compounds such as benzoic acid, p-(dimethylamino) benzoic acid, and hydroquinone (Imtiaz et al. 2022). When ring opening occurs, these intermediates turn into simple organic acids and produce CO_2 and H_2O (Imtiaz et al. 2022; He et al. 2023).

Plasma treatment has been widely demonstrated to enhance the decolorization and degradation of MG dye in aqueous solutions through various mechanisms and system configurations. For example, a gas-phase discharge-based non-thermal plasma system achieved a decolorization efficiency of 99.74% under optimized conditions, while the addition of potassium persulfate promoted sulfate radical generation, enabling 96% removal within just 10 minutes (Kumar et al. 2025). This underscores the role of catalytic oxidants in accelerating the degradation process. Similarly, pulsed discharge plasma applied on the water surface system (WSP), when combined with Fe^{2+} and peroxymonosulfate (PMS), reached a degradation efficiency of 97.9% for MG and improved energy efficiency by 9.7% compared to WSP alone (Hua et al. 2024). In these systems, active species such as hydroxyl radicals and sulfate radicals were key drivers of MG breakdown, emphasizing the critical role of reactive species in plasma-based dye removal. These findings align with the present study, supporting plasma treatment as a viable and effective approach for mitigating the environmental impact of synthetic dyes in wastewater.

Correlation Between Dye Decolorization Efficiency and Physicochemical Changes in Direct Plasma-Treated Dye Solutions

The strong relationship between dye decolorization efficiency and the observed changes in pH, electrical conductivity, TDS, and DO following plasma treatment can be attributed to the chemical and physical transformations induced by non-thermal plasma. During treatment, the plasma generates a variety of reactive oxygen and nitrogen species, including hydroxyl radicals (·OH) and ozone (O_3), which play a crucial role in the decolorization and structural modifications of dye molecules. These oxidative processes not only enhance dye decolorization but also alter the physicochemical properties of the aqueous solution, resulting in measurable changes in pH, conductivity, TDS, and DO (Karimian et al. 2025).

Figure 5 presents the changes in pH (Figure 5a) and electrical conductivity (Figure 5b) of the dye aqueous solutions after exposure to the plasma plume for varying treatment durations. The natural orange and MG dye solutions initially showed a pH of 7.55 ± 0.01 and 4.73 ± 0.31, respectively. The lowest pH values, both of which were statistically significant from their respective initial values, were observed after 45 min of direct plasma treatment, reaching 7.04 ± 0.04 and 3.74 ± 0.01 for the natural orange dye and MG solutions, respectively. This treatment duration also corresponded to the highest dye removal efficiencies achieved for both solutions. The observed pH reduction reflects the interaction between reactive species and the dye molecules during plasma treatment. Reactive oxygen and nitrogen species generated by plasma can dissolve into the solution and form potent acids, accelerating dye decolorization and structural transformations (Vasu et al. 2020; Kumar et al. 2022; Quispe-Quispe et al., 2024).

The electrical conductivity of the natural orange and MG solutions increased significantly, reaching final values of 596.67 ± 5.77 µS/cm and 190.00 ± 0.00 µS/cm, respectively, after 45 minutes of direct treatment compared with their initial conductivities of 430 µS/cm and 128 µS/cm. The conductivity increase indicates the accumulation of ions in the solution due to plasma discharge. A higher ion concentration provides more charge carriers, thereby enhancing conductivity. Longer treatment times result in greater ion deposition, further increasing conductivity (Thirumdas et al. 2018).

The highest TDS values were recorded after 45 minutes of direct plasma treatment (Figure 5c): initial values were 200 ppm for natural orange dye and 52 ppm for MG. The natural orange dye solution exhibited a maximum TDS of 344 ± 2.00 ppm, whereas the MG dye solution reached 157.33 ± 2.52 ppm. This statistically significant increase indicates a greater presence of dissolved ions in the solution with prolonged treatment, consistent with the observed rise in nitrate and nitrite concentrations (Pal et al. 2024).

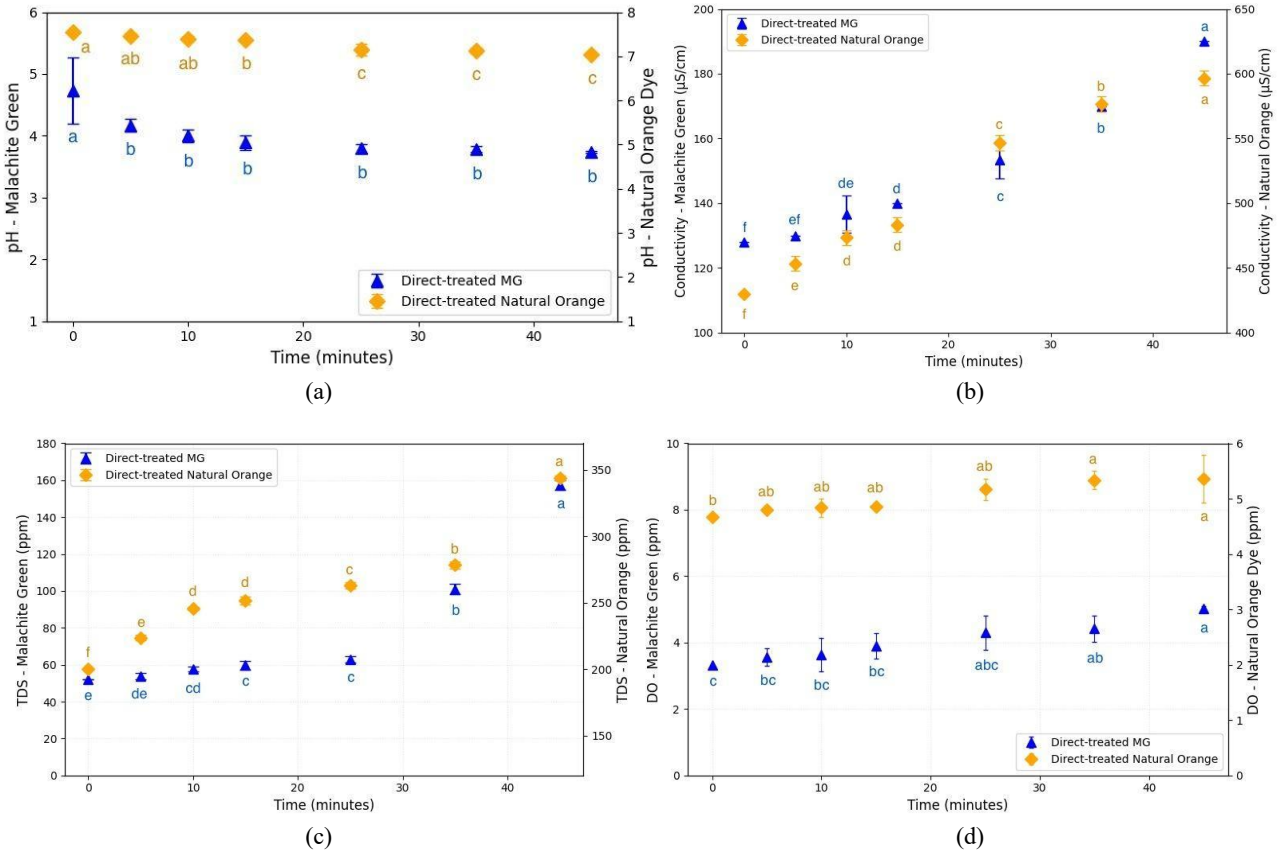

Figure 5: (**a**) pH, (**b**) conductivity, (**c**) TDS, and (**d**) DO of direct-treated natural orange and MG dye aqueous solutions

In terms of DO (Figure 5d), both dye solutions exhibited a statistically significant increase following plasma treatment, although the overall changes were relatively modest. The MG and natural orange dye solutions initially showed DO concentrations of 3.33 ppm and 4.66 ppm, respectively. After 45 minutes of treatment, these values increased only modestly to 5.03 ± 0.08 ppm for MG and 5.36 ± 0.43 ppm for the natural orange dye solution. The modest increase in DO observed in dye solutions treated with plasma can be attributed to the spatial localization and rapid consumption of reactive species generated at the plasma–liquid interface (Inagaki and Sasaki 2021). Plasma–liquid interactions produce a complex mixture of RONS with high oxidation potentials that readily react with dye molecules, thereby promoting efficient decolorization and structural modifications. However, many of these oxidants are short-lived and undergo rapid recombination or secondary reactions, limiting their contribution to a measurable and sustained increase in bulk dissolved oxygen concentration (Kumar 2023). Furthermore, the concurrent acidification of the solution and the observed increase in electrical conductivity during plasma treatment suggest the formation of nitric and nitrous species, along with other ionic byproducts. These physicochemical transformations facilitate the continuous consumption and conversion of dissolved oxygen into reactive intermediates, thereby preventing its accumulation in the aqueous phase (Sah et al. 2023). The dynamic interplay between reactive species generation, rapid oxidation of dye molecules, and secondary chemical processes accounts for the limited net increase in dissolved oxygen despite active plasma-induced oxidation.

Overall, the interplay among pH, electrical conductivity, TDS, and DO reflects the extent of dye decolorization and possible structural modifications occurring during plasma treatment. Higher dye decolorization efficiencies are associated with more pronounced changes in these water quality parameters, indicating the occurrence of active oxidative reactions and the progressive breakdown of complex dye molecules. These transformations lead to the formation of simpler intermediates and, ultimately, more stable and less harmful end products, demonstrating the effectiveness of plasma-induced oxidation in the remediation of dye-contaminated water (Fahmy et al. 2020; Karimian et al. 2025).

Dye Decolorization Efficiency of Indirect Plasma Treatment using PAW

As shown in Figure 6, indirect plasma treatment using PAW resulted in a statistically significant increase in dye decolorization efficiency for both dye solutions when evaluated relative to their respective initial concentrations. The initial concentrations (C_0) of the natural orange dye and MG solutions were 329 ppm and 74 ppm, respectively. These concentrations account for the 1:1 dilution applied when mixing dye solution with PAW, and were determined from absorbance measurements using Equation 2 and the respective calibration curves. For natural orange dye and MG solutions, the maximum observed decolorization efficiencies of 24.90 ± 1.35% and 19.20 ± 2.60%, respectively, were achieved with 60 minutes of PAW treatment. As shown in Figure 7, the color changes in the dye solutions after 10 days of storage across the different PAW treatment durations were minimal.

Meanwhile, based on the degradation pathways previously proposed, long-lived reactive species in PAW, including H_2O_2, NO_2^-, and H^+, contribute to dye degradation primarily through the formation of peroxynitrous acid (ONOOH) under acidic conditions. ONOOH, a potent oxidizing agent with an oxidation potential of 2.0 V, effectively facilitated the breakdown of the chemical structures of both dyes. In addition, hydrogen peroxide (H_2O_2), with an oxidation potential of 1.77 V, together with short-lived hydroxyl radicals (•OH), likely attacked the chemical bonds within the dye molecules, further promoting degradation (Kumar et al. 2022).

The PAW treatment proved more effective in decolorizing natural orange dye than MG, which can be attributed to the comparatively simpler molecular structure of annatto-derived pigments. Annatto dye is composed mainly of bixin and norbixin, both featuring a carotenoid backbone with multiple conjugated double bonds. This structural arrangement, while imparting color, also makes the

molecules more vulnerable to oxidative attack by the long-lived reactive species in PAW. As a result, potential oxidative degradation proceeds more readily in natural orange dye than in the structurally more complex MG, leading to higher decolorization efficiency and potential structural transformations.

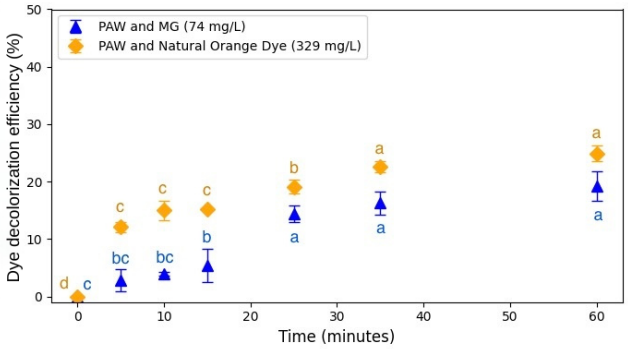

Figure 6: Dye decolorization efficiency of PAW for natural orange and MG aqueous solutions

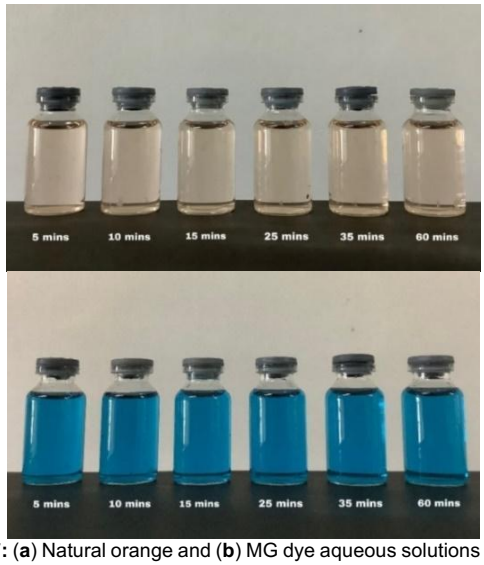

Figure 7: (**a**) Natural orange and (**b**) MG dye aqueous solutions following indirect plasma treatment after 10 days of storage

The above-mentioned long-lived ROS and RNS present in PAW, which are responsible for dye decolorization and potential structural transformations during the indirect treatment, along with their possible individual reaction pathways, are presented below (Vasu et al., 2020; Kumar et al., 2022).

$$\cdot OH + \cdot OH \rightarrow H_2O_2 \text{ (Hydrogen Peroxide)}$$
$$2NO_2 + H_2O \rightarrow NO_3^- + NO_2^- + 2H^+ \text{ (Nitrate)}$$
$$NO + \cdot OH \rightarrow NO_2^- \text{ (Nitrite)}$$
$$O + O_2 + M \rightarrow O_3 + M \text{ (Ozone)}$$

The indirect method involved a 1:1 dilution ratio and was evaluated only after 10 days of storage. In this method, only long-lived species such as hydrogen peroxide, nitrate, and nitrite remained, which, although still reactive, acted more slowly and with lower oxidative potential. This resulted in dye decolorization efficiencies of a maximum of 24.90 ± 1.35% and 19.20 ± 2.60% with 60 minutes of PAW treatment for natural orange dye and MG solutions, respectively.

Decolorization Kinetic Models of Direct Plasma-Treated Dye Solutions

Kinetic analyses of the decolorization of directly treated natural orange dye and MG were performed using zero-order, first-order, and second-order kinetic models as shown in Figures 8 and 9, respectively. These models were selected because they are among the most widely used approaches for evaluating the decolorization and structural modifications of organic pollutants in advanced oxidation processes, including plasma-based water treatment systems. Additionally, they provide a basis for assessing the relationship between dye concentration and decolorization rate, thereby facilitating the identification of the kinetic behavior that best describes the plasma-induced decolorization of the dyes (Jiang and Zheng 2013; El-Tayeb et al. 2021; Karimian et al. 2025; Mohammed et al. 2023; Yin et al. 2014). Zero-order kinetics implies that the decolorization rate remains constant and is independent of the dye concentration. This model implies a constant degradation rate regardless of dye concentration and may be applicable under conditions where reactive species are present in excess or when the degradation process is limited by factors other than dye concentration (El-Tayeb et al. 2021). In contrast, first-order kinetics assumes that the decolorization rate is directly proportional to the dye concentration, indicating that the reaction proceeds more slowly as the dye concentration decreases over time (Yin et al. 2014). Second-order kinetics suggests that the decolorization rate depends on the interaction between two reacting species, such as the dye and a catalyst or another reactive species, making the rate proportional to the product of their concentrations.

The correlation coefficients (R^2) for the natural orange dye were 0.7293, 0.9271, and 0.9555 for the zero-, first-, and second-order models, respectively. Similarly, the R^2 values for MG were 0.5234, 0.7302, and 0.9312 for the zero-, first-, and second-order models, respectively. On the other hand, the best-fit line for the natural orange dye is expressed by the equation $y = 0.0003x - 0.0011$ ($R^2 = 0.9555$), while for MG, the corresponding fit line is $y = 0.0036x + 0.0057$ ($R^2 = 0.9312$). Numerous studies have reported that organic dye decolorization during plasma treatment followed first-order kinetics (Jiang and Zheng 2013; Yin et al. 2014; El-Tayeb et al. 2021; Karimian et al. 2025). In contrast, the present study found that the decolorization of malachite green (MG) and annatto orange dye was better described by a second-order kinetic model. Nevertheless, second-order kinetics has also been reported in the literature for certain plasma-based dye treatment systems. For instance, in the oxidative removal of azo and non-azo dyes using a gas–liquid interface non-thermal plasma reactor, the second-order kinetic model provided a better fit to the experimental data than the zero-order and first-order models, yielding high correlation coefficients ($R^2 = 0.86–0.99$) (Mohammed et al. 2023). The applicability of the second-order model suggests that the decolorization or degradation rate may depend not only on the dye concentration but also on the concentration of reactive species generated during plasma treatment (Vasikaran et al. 2022). These findings indicate that second-order kinetics can effectively describe plasma-induced dye decolorization or degradation under certain treatment conditions and reactor configurations.

Determination of the kinetics of plasma-induced dye decolorization is essential for elucidating the underlying degradation mechanisms and optimizing process performance. Kinetic models provide a quantitative framework for describing the temporal evolution of dye concentration during plasma treatment and for evaluating the efficiency of the decolorization process. Furthermore, kinetic analysis enables the prediction of treatment performance under different operating conditions, including applied voltage, gas flow rate, and treatment time. Such information is fundamental for optimizing process parameters, comparing reactor performance, and facilitating the design, scale-up, and practical implementation of plasma-based technologies for wastewater treatment (Jiang and Zheng 2013; Yin et al. 2014; Kasih et al. 2018).

The half-lives of natural orange (4.44 minutes) and malachite green (2.81 minutes) dyes were calculated using $t_{1/2} = 1/(k[C_0])$. Both the rate constants (k in $ppm^{-1}\ min^{-1}$) and initial concentrations (C_0 in ppm) were expressed in compatible ppm-based units. Specifically, k values of 0.0003 $ppm^{-1}\ min^{-1}$ for natural orange and 0.0036 $ppm^{-1}\ min^{-1}$ for MG, as derived from their respective fit lines, were applied to their respective concentrations of 750 ppm and 100 ppm.

The shorter half-life of MG (2.81 minutes) compared to that of natural orange dye (4.44 minutes) further supports its faster decolorization or possible degradation under direct plasma treatment. These findings demonstrate that direct plasma treatment is more efficient for degrading MG, leading to a more rapid reduction in its concentration.

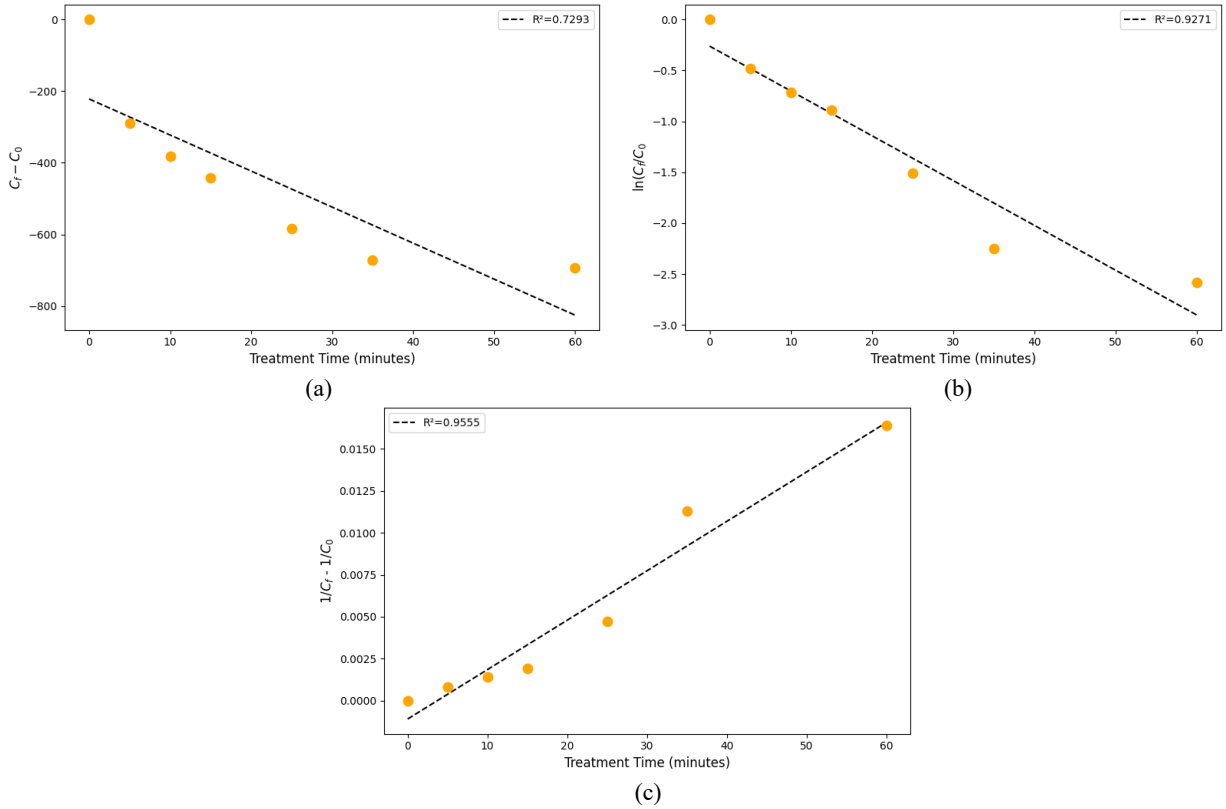

Figure 8: (**a**) Zero, (**b**) first, and (**c**) second order kinetic model of natural orange dye decolorization with respect to treatment time

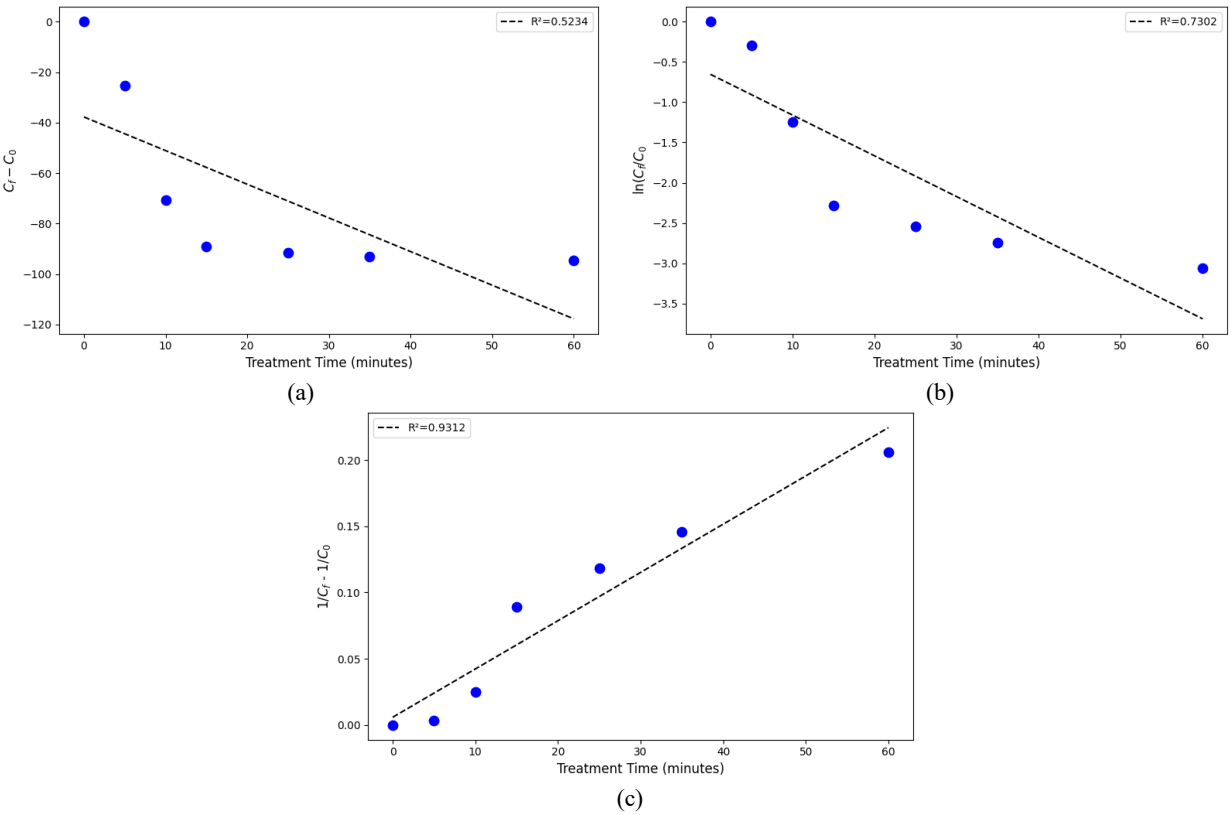

Figure 9: (**a**) Zero, (**b**) first, and (**c**) second order kinetic model of MG degradation with respect to treatment time

CONCLUSION

This study demonstrated the decolorization of MG and natural orange dye using direct atmospheric pressure plasma jet (APPJ) exposure and indirect treatment using plasma-activated water (PAW). The highest PAW-induced decolorization efficiencies of $24.90 \pm 1.35\%$ for natural orange dye and $19.20 \pm 2.60\%$ for malachite green were achieved using 60-minute PAW, highlighting the role of long-lived reactive species, consistent with physicochemical changes observed in pH, conductivity, TDS, and DO. Meanwhile, decolorization efficiencies of $92.47 \pm 1.29\%$ for natural orange dye and $95.32 \pm 0.29\%$ for MG after 45 minutes were observed in direct plasma treatment. These results are consistent with the presence of both short- and long-lived species and are consistent with observed physicochemical changes. Kinetic analyses revealed that both MG and natural orange dye followed second-order kinetics. This indicates that their decolorization rate is concentration-dependent and involves interactions between dye molecules and reactive plasma species. Overall, these findings demonstrate that APPJ-based systems provide an effective and environmentally sustainable approach for the remediation of dye wastewater.

ACKNOWLEDGMENTS

The authors extend their sincerest gratitude to the Plasma Science and Technology research group and the Department of Physical Sciences, University of the Philippines Baguio, for generously providing laboratory space for this study.

CONFLICT OF INTEREST

The authors have no conflicts of interest to declare that are relevant to the content of this article.

CONTRIBUTIONS OF INDIVIDUAL AUTHORS

DBS contributed to the conceptualization, methodology, formal analysis, investigation, and preparation of the original draft. MMMR contributed to the conceptualization, methodology, formal analysis, as well as the review and editing of the manuscript. GMM contributed to the conceptualization and methodology.

REFERENCES

Aluko E. Ethanol-based extraction of annatto (*Bixa orellana* L.) and characterization of the bixin and norbixin. ACS Omega 2024; 9(16):18273-18277.

Attri P, Yusupov M, Park JH, Lingamdinne LP, Koduru JR, Shiratani M, Bogaerts A. Mechanism and comparison of needle-type non-thermal direct and indirect atmospheric pressure plasma jets on the degradation of dyes. Scientific Reports 2016; 6(1):34419.

Baculi RQ, Malapit GM, Abayao LE. Atmospheric pressure plasma deposition of silver nanoparticles on bark fabric for bacterial growth inhibition. The Journal of The Textile Institute 2023; 114(1):142-150.

Bhandari NL, Pokhrel B, Bhandari U, Bhattarai S, Devkota A, Bhandari G. An overview of research on plant based natural dyes in Nepal: scope and challenges. Journal of Agriculture and Natural Resources 2020; 3(2):45-66.

Cruz-Lacierda ER, De la Peña LD, Lumanlan-Mayo S. The use of chemicals in aquaculture in the Philippines. In: Use of chemicals in aquaculture in Asia. Iloilo: Southeast Asian Fisheries Development Center 2000:155-184.

Devi M, Ariharan VN, Prasad N. Annato: eco-friendly and potential source for natural dye. International Research Journal of Pharmacy 2013; 4(6):106-108.

El-Tayeb A, El-Dein AZ, Elnaggar AY, Hussein EE. Influence of temperature in degradation of organic pollution using corona discharge plasma. Sustainability 2021; 13(23):12971.

Fahmy A, El-Zomrawy A, Saeed AM, Sayed AZ, Ezz El-Arab MA, Shehata H, Friedrich J. Degradation of organic dye using plasma discharge: optimization, pH and energy. Plasma Research Express 2020; 2(1):015009.

Gallardo Cabrera C, Rojas Barahona ÁF. Stability study of an aqueous formulation of the annatto dye. International Food Research Journal 2015; 22(5):2149–2154.

He J, Mo P, Luo YS, Yang PH. Strategies for solving the issue of malachite green residues in aquatic products: a review. Aquaculture Research 2023; 2023(1):8578570.

Hua W, Kang Y, Yuan H. Efficient degradation of emerging pollutant-malachite green in water by pulsed discharge plasma on water surface in cooperation with Fe^{2+}/PMS. Environmental Pollution 2024; 359:124773.

Imtiaz T, Shah A, Ullah N, Iftikhar FJ, Shah I, Shah SM, Shah SS. Electrochemical nanosensor for ultrasensitive detection of malachite green and monitoring of its photocatalytic degradation. npj Clean Water 2022; 5(1):69.

Inagaki Y, Sasaki K. Reaction frequency of solvated electrons in water interacting with atmospheric-pressure helium plasma jet. Japanese Journal of Applied Physics 2021; 60(9):096001.

Jiang B, Zheng JT. Electrical plasma technology for dye decolorization in a continuous reactor system. Advanced Materials Research 2013; 726:2169-2172.

Jitsomboonmit P, Nisoa M, Dangtip S. Experimental study of current-voltage characteristics and optical emission of various gases in dielectric barrier discharge at atmospheric pressure. Physics Procedia 2012; 32:723-731.

Karimian S, Shariat M, Mashayekhi H. Deep insight into methyl blue decolorization using non-thermal pulsed plasma: experimental and modeling approaches. Scientific Reports 2025; 15(1):32989.

Kasih TP, Kharisma A, Perdana MK, Pontororing PP, Mangindaan D. Influence of admixing oxygen on Ar plasma discharge for organic pollutant degradation in wastewater treatment. IOP Conference Series: Earth and Environmental Science 2018; 195(1):012076.

Kumar A. Design, development and characterization of atmospheric plasma system for wastewater treatment. University of Belgrade (Serbia) 2023.

Kumar A, Škoro N, Gernjak W, Povrenović D, Puač N. Direct and indirect treatment of organic dye (Acid blue 25) solutions by using cold atmospheric plasma jets. Frontiers in Physics 2022; 10:835635.

Kumar P, Saxena P. Plasma-Activated Water (PAW) for the degradation of organic pollutants in diluted industrial effluents. arXiv 2026; arXiv:2601.01270.

Kumar TN, Mohapatro S, Dash RR. Gas phase discharge based non-thermal plasma system for the removal of malachite green dye. 2025 IEEE Industry Applications Society Annual Meeting (IAS) 2025; June:1-8. IEEE.

Malapit GM, Baculi RQ. Bactericidal efficiency of silver nanoparticles deposited on polyester fabric using atmospheric pressure plasma jet system. The Journal of The Textile Institute 2022; 113(9):1878-1886.

Mohammed SA, Al-Khazrajy OS, Abdallh M, Aadim KA, Al-Mamari A, Al-Owaisi H, Yousif E. Removal of dyes from aqueous solutions using non-thermal plasma. Environmental Processes 2023; 10(4):63.

National Toxicology Program. Toxicology and carcinogenesis studies of malachite green chloride and leucomalachite green (CASRNs 569-64-2 and 129-73-7) in F344/N rats and B6C3F1 mice (feed studies). Research Triangle Park (NC): National Institute of Environmental Health Sciences; 2005. (NTP Technical Report No. 527)

Navrátil Z, Trunec D, Šmíd R, Lazar L. A software for optical emission spectroscopy–problem formulation and application to plasma diagnostics. Czechoslovak Journal of Physics 2006; 56(S2). doi:10.1007/s10582-006-0308-y.

Oladoye PO, Ajiboye TO, Wanyonyi WC, Omotola EO, Oladipo ME. Ozonation, electrochemical, and biological methods for the remediation of malachite green dye wastewaters: a mini review. Sustainable Chemistry for the Environment 2023; 3:100033.

Ouzar A, Goutomo BT, Nam K, Kim IK. Enhanced removal of malachite green from wastewater using nonthermal plasma gliding arc discharge combined with ferrate oxidation. Desalination and Water Treatment 2024; 320:100743.

Pal P, Pal UN, Singh V, Sharma NK, Singh M, Mishra A, Lamba RP. Experimental investigation for the generation and characterization of plasma-activated water. IEEE Transactions on Plasma Science 2024.

Pattnaik P, Dangayach GS, Bhardwaj AK. A review on the sustainability of textile industries wastewater with and without treatment methodologies. Reviews on Environmental Health 2018; 33(2):163-203.

Peramune D, Manatunga DC, Dassanayake RS, Premalal V, Liyanage RN, Gunathilake C, Abidi N. Recent advances in biopolymer-based advanced oxidation processes for dye removal applications: a review. Environmental Research 2022; 215:114242.

Pineda EJT, Rubio MMM, Malapit GM. Atmospheric pressure plasma treatment of pure cotton textile for improved hydrophilicity and optimized dyeability via response surface methodology. SciEnggJ 2025; 18(2):304–319.

Quispe-Quispe A, Pérez-Falcón LF, Quispe-Marcatoma J, Landauro CV, Peña Rodriguez VA. Removal of cochineal dye color through atmospheric pressure plasma discharge jet. Applied Sciences 2024; 14(2):680.

Sah AK, Al-Amin M, Talukder MR. DC magnetic field–assisted improvement of textile dye degradation efficiency with multi-capillary air bubble discharge plasma jet. Environmental Science and Pollution Research 2023; 30(30):74877–74888.

Silva ER, Dall'Oglio EL, Vasconcelos LG, Morais EB. Decolorization of the benzidine-based azo dye Congo red by the new strain *Shewanella xiamenensis* G5-03. Brazilian Journal of Biology 2021; 82:e237386.

Thirumdas R, Kothakota A, Annapure U, Siliveru K, Blundell R, Gatt R, Valdramidis VP. Plasma activated water (PAW): Chemistry, physico-chemical properties, applications in food and agriculture. Trends in Food Science & Technology 2018; 77:21-31.

Vasikaran EM, Murugesan P, Moses JA, Anandharamakrishnan C. Performance of non-thermal plasma reactor for removal of organic and inorganic chemical residues in aqueous media. Journal of Electrostatics 2022; 115:103671.

Vasu D, Ramkumar M, Arunkumar A, Pandiyaraj KN. Cold atmospheric pressure argon plasma jet assisted degradation of malachite green (MG) aqueous solution. Frontiers in Advanced Materials Research 2020; 2:51-61.

Ventosa E. Bixa Orellana (annatto). CABI Compendium. 2016 Jun 9; doi:10.1079/cabicompendium.9242

Wang Q, Liang L, Tian G, Mao Q, Meng X. Adsorption of azo dye malachite green onto rice wine lees: kinetic and adsorption isotherms. Nature Environment and Pollution Technology 2020; 19(2):563-570.

Wang X, Jiang J, Gao W. Reviewing textile wastewater produced by industries: characteristics, environmental impacts, and treatment strategies. Water Science and Technology 2022; 85(7):2076-2096.

Yin H, Xiong L, Jiang B, Zheng J, Xue Q. Non-thermal plasma technology for methylene blue decolorization in continuous and circulating system: kinetic model and reactor performance. Journal of Advanced Oxidation Technologies 2014; 17(2):265-281.

Younis SA, Serp P, Nassar HN. Photocatalytic and biocidal activities of $ZnTiO_2$ oxynitride heterojunction with MOF-5 and g-C_3N_4: A case study for textile wastewater treatment under direct sunlight. Journal of Hazardous Materials 2021; 410:124562.

Zhou R, Zhou R, Wang P, Xian Y, Mai-Prochnow A, Lu X, Bazaka K. Plasma-activated water: generation, origin of reactive species and biological applications. Journal of Physics D: Applied Physics 2020; 53(30):303001.